Electron Injection into Plasma Wake Fields by Colliding Laser Pulses

E. Esarey,[1] R. F. Hubbard,[1] W. P. Leemans,[2] A. Ting,[1] and P. Sprangle[1]

[1]*Beam Physics Branch, Plasma Physics Division, Naval Research Laboratory, Washington, D.C. 20375-5346*
[2]*Ernest Orlando Lawrence Berkeley National Laboratory, University of California at Berkeley, Berkeley, California 94720*

An injector and accelerator is analyzed that uses three collinear laser pulses in a plasma: an intense pump pulse, which generates a large wake field ($\gtrsim 20$ GV/m), and two counterpropagating injection pulses. When the injection pulses collide, a slow phase velocity beat wave is generated that injects electrons into the fast wake field for acceleration. Particle tracking simulations in 1D with injection pulse intensities near 10^{17} W/cm^2 indicate the production of relativistic electrons with bunch durations as short as 3 fs, energy spreads as small as 0.3%, and densities as high as 10^{18} cm^{-3}. [S0031-9007(97)04154-9]

PACS numbers: 52.40.Nk, 41.75.Lx, 52.75.Di

Plasma-based accelerators [1] may provide a compact source of high energy electrons due to their ability to sustain ultrahigh electric fields E_z on the order of $E_0 = cm\omega_p/e \simeq n_0^{1/2}[\text{cm}^{-3}]$ V/cm, where $\omega_p = (4\pi n_0 e^2/m)^{1/2}$ is the plasma frequency and n_0 is the plasma density. Accelerating fields of 10–100 GV/m have been generated over distances of a few millimeters [2–4] in both the standard [5] and self-modulated [6,7] regimes of the laser wake-field accelerator (LWFA). The characteristic scale length of the accelerating plasma wave is the plasma wavelength $\lambda_p = 2\pi c/\omega_p$, which is typically $\lesssim 100$ μm. Although several recent experiments [3,4] have demonstrated the self-trapping and acceleration of plasma electrons in the self-modulated LWFA, the production of electron beams with relatively low momentum spread and good pulse-to-pulse energy stability will require injection of ultrashort electron bunches into the wake field with femtosecond timing accuracy. These requirements are beyond the current state-of-the-art performance of photocathode radio-frequency electron guns.

Recently an all-optical method for injecting electrons in a standard LWFA has been proposed [8] that utilizes two laser pulses which propagate either perpendicular or parallel to one another. The first pulse (pump pulse) generates the wake field, and the second pulse (injection pulse) intersects the wake some distance behind the pump pulse. The ponderomotive force $F_p \sim \nabla a^2$ of the injection pulse can accelerate a fraction of the plasma electrons such that they become trapped in the wake field, where $a^2 \simeq 7 \times 10^{-19}\lambda^2[\mu\text{m}]I[\text{W/cm}^2]$, $\lambda = 2\pi c/\omega$ is the laser wavelength, and I is the intensity. Simulations, which were performed for ultrashort pulses at high densities ($\lambda_p/\lambda = 10$ and $E_z/E_0 = 0.7$), indicated the production of a 10 fs, 21 MeV electron bunch with a 6% energy spread. However, high intensities ($I > 10^{18}$ W/cm^2) are required in both the pump and injection pulses ($a \simeq 2$). An all-optical electron injector would be a significant step in reducing the size and cost of a LWFA.

In the following, a colliding pulse optical injection scheme for a LWFA is proposed and analyzed that uses three short laser pulses: an intense pump pulse (denoted by subscript 0), a forward going injection pulse (subscript 1), and a backward going injection pulse (subscript 2), as shown in Fig. 1. The frequency, wave number, and normalized intensity are denoted by, respectively, ω_i, k_i, and a_i ($i = 0, 1, 2$). Furthermore, $\omega_1 = \omega_0$, $\omega_2 = \omega_0 - \Delta\omega$ ($\Delta\omega \geq 0$), and $\omega_0 \gg \Delta\omega \gg \omega_p$ are assumed such that $k_1 = k_0$ and $k_2 \simeq -k_0$. The pump pulse generates a fast ($v_{p0} \simeq c$) wake field. When the injection pulses collide (some distance behind the pump) they generate a slow ponderomotive beat wave with a phase velocity $v_{pb} \simeq \Delta\omega/2k_0$. During the time in which the two injection pulses overlap, a two-stage acceleration process can occur; i.e., the slow beat wave injects plasma electrons into the fast wake field for acceleration to high energies. It will be shown that injection and acceleration can occur at low densities ($\lambda_p/\lambda \sim 100$), thus allowing for high single-stage energy gains, with normalized injection pulse intensities of $a_1 \sim a_2 \sim 0.2$, i.e., 2 orders of magnitude less intensity than required in Ref. [8]. Furthermore, the colliding pulse concept offers detailed control of the injection process: The injection phase can be controlled via the position of the forward injection pulse, the beat phase
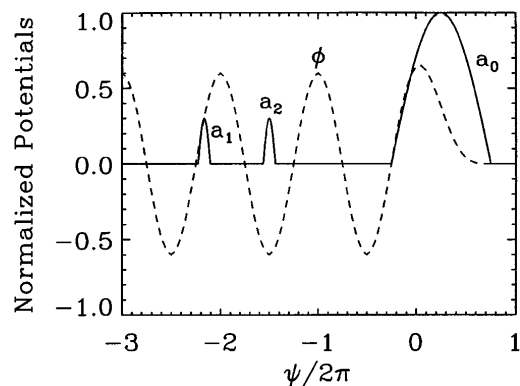

FIG. 1. Profiles of the pump laser pulse a_0, the wake ϕ, and the forward a_1 injection pulse, all of which are stationary in the $\psi = k_p(z - v_{p0}t)$ frame, and the backward injection pulse a_2, which moves to the left at $\simeq 2c$.

velocity via $\Delta\omega$, the injection energy via the pulse amplitudes, and the injection time (number of trapped electrons) via the backward pulse duration.

A somewhat analogous two-stage acceleration process can lead to self-trapping in the self-modulated LWFA due to the interaction of the Raman backscatter (RBS) waves with the wake field [4,9,10]. In the self-modulated LWFA [6,7], the plasma density n_0 is sufficiently high ($\lambda_p/\lambda \sim 10$) such that $L > \lambda_p$, where L is the laser pulse length. Since $L > \lambda_p$, RBS readily occurs, which involves the decay of the pump laser light (ω, k) into backward light $(\omega - \omega_p, -k)$ and a plasma wave $(\omega_p, 2k)$ [1]. The slow $(v_p = \omega_p/2k)$ RBS plasma wave can preheat the plasma such that a fraction of the electrons are accelerated to high energies in the fast $(v_p \simeq c)$ wake field [4,9,10]. Dephasing limits the electron energy gain to $W_d \simeq 4mc^2\lambda_p^2 E_z/\lambda^2 E_0 \sim n_0^{-1}$, which is relatively low ($W_d \sim 100$ MeV) at high densities [1]. Higher single-state energy gains can be obtained at lower plasma densities as in the standard LWFA [5], in which $L \simeq \lambda_p$ ($\lambda_p/\lambda \sim 100$). Since $L \simeq \lambda_p$, Raman instabilities will be suppressed and self-trapping of plasma electrons is unlikely. Acceleration in the standard LWFA requires an additional injection mechanism.

The colliding pulse injection mechanism will be analyzed in 1D with the plasma wave and laser fields represented by the normalized scalar $\phi = e\Phi/mc^2$ and vector $\mathbf{a} = e\mathbf{A}_\perp/mc^2$ potentials, respectively. The axial component of the normalized electron momentum $u_z = p_z/mc = \gamma\beta_z$ obeys

$$\frac{du_z}{dct} = \frac{\partial\phi}{\partial z} - \frac{1}{2\gamma}\frac{\partial a^2}{\partial z}, \qquad (1)$$

where $\gamma = \gamma_z\gamma_\perp$, $\gamma_\perp = (1 + a^2)^{1/2}$, and $\gamma_z = (1 - \beta_z^2)^{-1/2}$. In terms of the phase of the electron with respect to the wake field $\psi = k_p(z - v_{p0}t)$, Eq. (1) is

$$\frac{d^2\psi}{d\tau^2} = \frac{(1 - \beta_z^2)}{\gamma}\frac{\partial\phi}{\partial\hat{z}} - \frac{1}{\gamma^2}\left(\frac{\partial}{\partial\hat{z}} + \beta_z\frac{\partial}{\partial\tau}\right)\frac{a^2}{2}, \quad (2)$$

where $k_p = \omega_p/c$, $v_{p0} = c\beta_{p0}$ is the wake-field phase velocity, $\hat{z} = k_p z$, $\tau = \omega_p t$, and $\beta_z = d\psi/d\tau + \beta_{p0}$.

The effects of three waves will be considered: a plasma wake field $\phi = \hat{\phi}(\psi)\cos\psi$, and a forward and a backward injection laser pulse, both of the form $\mathbf{a}_i = \hat{a}_i(z - v_{gi}t)(\sin\theta_i\mathbf{e}_x + \cos\theta_i\mathbf{e}_y)$. Here, $\theta_i = k_i z - \omega_i t$ and the amplitudes $\hat{a}_i$ and $\hat{\phi}$ are assumed to be slowly varying compared to the phases θ_i and ψ. Also, k_i and ω_i satisfy $k_i = \sigma_i\omega_i(1 - \omega_p^2/\omega_i^2)^{1/2}$, where $\sigma_1 = 1$ and $\sigma_2 = -1$, which implies a group velocity $v_{gi} = c\beta_{gi} = c^2k_i/\omega_i$ ($v_{p0} = v_{g0} = v_{g1}$). Furthermore, $a^2 = \hat{a}_1^2 + \hat{a}_2^2 + 2\hat{a}_1\hat{a}_2\cos\psi_b$, where $\psi_b = \theta_1 - \theta_2 = \Delta k(z - v_{pb}t)$ is the beat phase, $v_{pb} = c\beta_{pb} = \Delta\omega/\Delta k$, and $\Delta k = k_1 - k_2 \simeq 2k_0$. To leading order, Eq. (2) becomes

$$d^2\psi/d\tau^2 \simeq b_0\hat{\phi}\sin\psi + b_1(\Delta k/k_p)\hat{a}_1\hat{a}_2\sin\psi_b, \quad (3)$$

where $b_0 = -\gamma_\perp^{-1}(1 - \beta_z^2)^{3/2}$, $b_1 = \gamma_\perp^{-2}(1 - \beta_z^2)(1 - \beta_{pb}\beta_z)$, and $\psi_b = [(\beta_{p0} - \beta_{pb})\tau + \psi]\Delta k/k_p$.

In the absence of the injection pulses, electron motion in the wake field is described by the Hamiltonian [11] $H_w = \gamma - \beta_{p0}(\gamma^2 - 1)^{1/2} - \phi$, where $\phi = \phi_0\cos\psi$. The boundary between trapped and untrapped orbits is given by the separatrix $H_w(\gamma, \psi) = H_w(\gamma_{p0}, \pi)$, where $\gamma_{p0} = (1 - \beta_{p0}^2)^{-1/2}$. The minimum momentum of an electron on the separatrix is $u_{\min} \simeq (1/\Delta\phi - \Delta\phi)/2$, where $\Delta\phi = \phi_0(1 + \cos\psi)$, assuming $\gamma_{p0}\Delta\phi \gg 1$ and $\beta_{p0} \simeq 1$. In particular at $\psi = 0$, $u_{\min} = 0$ for $\phi_0 = \frac{1}{2}$, which means that an electron that is at rest at the phase $\psi = 0$ will be trapped. The background plasma electrons, however, are untrapped and are undergoing a fluid oscillation with a momentum $u_f \simeq -\phi(\phi^2 \ll 1)$. Hence, at $\psi = 0$, the plasma electrons are moving backward with $u_f \simeq -\phi_0$, which is far from trapping.

The beat wave leads to formation of phase space buckets (separatrices) of width $2\pi/\Delta k \simeq \lambda_0/2$, which are much shorter than those of the wake field (λ_p), thus allowing for a separation of time scales. In particular, it can be shown that both the transit time $2\pi/\Delta\omega$ of an untrapped electron through a beat wave bucket and the synchrotron (bounce) time $\pi/(\hat{a}_1\hat{a}_2)^{1/2}\omega_0$ of a deeply trapped electron in a beat wave bucket are much shorter than a plasma wave period $2\pi/\omega_p$. Hence, on the time scale in which an electron interacts with a beat wave bucket, the wake field can be approximated as static.

In the combined fields, the electron motion can be analyzed in the local vicinity of a single period of the beat wave by assuming that the wake-field electric field $E_z = -k_p^{-1}E_0\partial\phi/\partial z \simeq E_{z0}$ is constant. The Hamiltonian associated with Eq. (3) is given by

$$H_b = \gamma - \beta_{pb}[\gamma^2 - \gamma_\perp^2(\psi_b)]^{1/2} + \epsilon\psi_b, \quad (4)$$

where $\epsilon = E_{z0}k_p/E_0\Delta k$ is constant and $\gamma_\perp^2 = 1 + \hat{a}_1^2 + \hat{a}_2^2 + 2\hat{a}_1\hat{a}_2\cos\psi_b$. When $\epsilon = 0$, the phase space orbits are symmetric with x points at $\beta_z = \beta_{pb}$, $\psi_b = \pm 2\pi j$ and o points at $\beta_z = \beta_{pb}$, $\psi_b = \pi \pm 2\pi j$ ($j = 0, 1, 2, \ldots$). When $\epsilon \neq 0$, the separatrix distorts into fish-shaped islands. When $\epsilon < 0$ ($\epsilon > 0$), the "fish tail" of the separatrix opens to the right (left). In terms of the axial momentum, the maximum and minimum points on the separatrix $(u_b)_m$, obtained from Eq. (4), are

$$(u_b)_m \simeq \beta_{pb}(\gamma_0 - \pi\gamma_{pb}^2|\epsilon|) \pm 2\hat{a}_1\gamma_{pb}$$
$$\times (1 - \pi\gamma_0|\epsilon|/2\hat{a}_1^2)^{1/2}, \qquad (5)$$

where $\gamma_0 = \gamma_{pb}(1 + 4\hat{a}_1^2)^{1/2}$, $\gamma_{pb} = (1 - \beta_{pb}^2)^{-1/2}$, $\pi\gamma_0|\epsilon|/2\hat{a}_1^2 < 1$, and $\hat{a}_1 = \hat{a}_2$ are assumed.

A scenario by which the beat wave leads to trapping in the plasma wave is the following. In the phase region $-\pi/2 < \psi < 0$, the plasma electrons are flowing backward, $u_f = -\phi_0\cos\psi < 0$, and the electric field is accelerating, $E_z/E_0 = \phi_0\sin\psi < 0$. Here $\epsilon < 0$ and the beat wave buckets open to the right. Consider an electron that is initially flowing backward and resides below the beat wave separatrix. Since the separatrix opens to the right, there exist open orbits which can take

an electron from below to above the beat wave separatrix. Such an electron, after interacting with one or more beat wave periods, can acquire a sufficiently large positive velocity to allow trapping and acceleration in the plasma wave. These open phase space orbits, which provide the necessary path for electron acceleration, can exist when the beat wave resides within $-\pi/2 \leq \psi \pm 2\pi j \leq 0$.

The threshold for injection into the wake field can be estimated by considering the effects of the wake field and the beat wave individually and by requiring that (i) the maximum energy of the beat wave separatrix exceeds the minimum energy of the wake-field separatrix $(u_b)_{\max} \geq (\Delta\phi^{-1} - \Delta\phi)/2$ and (ii) the minimum momentum of the beat wave separatrix be less than the plasma electron fluid momentum $(u_b)_{\min} \leq -\phi$, where $(u_b)_{\max}, (u_b)_{\min}$ are given by Eq. (5) with $\epsilon = 0$. These two conditions imply that the beat wave separatrix overlaps both the wake-field separatrix and the plasma fluid oscillation, thus providing a phase space path for plasma electrons to become trapped in the wake field. For a given wake-field amplitude ϕ_0, conditions (i) and (ii) imply the optimal phase location $3\phi_0 \cos\psi \simeq 3^{1/2} - 2\phi_0 - 2\beta_{pb}$ and threshold amplitude $6\hat{a}_1 > 3^{1/2} - 2\phi_0 + \beta_{pb}$ of the injection pulse, where $\phi_0^2 \cos^2\psi \ll 1$, $\hat{a}_1^2 \ll 1$, and $\beta_{pb}^2 \ll 1$ were assumed. For example, $\phi_0 = 0.6$ and $\beta_{pb} = 0.05$ imply $\psi = -1.3 - 2\pi j$ and $\hat{a}_1 > 0.11$.

To further evaluate the colliding laser injection method, the motion of test particles in the combined wake and laser fields was simulated by numerically solving Eq. (2). At $\tau = 0$, the forward (backward) pulse profile $\hat{a}_1$ ($\hat{a}_2$) is a half-period of a sine wave with maximum amplitude a_{1m} (a_{2m}), centered at $\psi = \psi_1 < 0$ ($\psi_2 > 0$), with length L_1 (L_2). Test particles are loaded uniformly within $0 \leq \psi \leq \psi_{\max}$ with $d\psi/d\tau = -\beta_{p0}$ (initially at rest) and pushed from $\tau = 0$ to $\tau = \tau_{\max}$. In Figs. 2 and 3, $\omega_1/\omega_p = 100$, $\omega_2/\omega_p = 90$, and $\phi_0 = 0.6$, which for $\lambda_1 = 2\pi c/\omega_1 = 1$ μm implies $n_0 \simeq 10^{17}$ cm^{-3} and $E_z = 0.6E_0 \simeq 19$ GV/m. Also, $\hat{\phi} = \phi_0[1 - \exp(-\psi^2/\pi^2)]$ for $\psi \leq 0$.

To validate the analytical predictions for the trapping thresholds, a "near threshold" case was simulated with $a_{1m} = a_{2m} = 0.3 (1.2 \times 10^{17}$ W/cm^2), $L_1 = L_2 = \lambda_p/8$ (42 fs), $\psi_1 = -13.6$ and $\psi_2 = 21.4$ (chosen so the beat wave and test particles overlap). Figure 2 shows a phase space plot (u_z versus ψ) of the trapped electrons at $\tau_{\max} = 300$ (0.48 cm). The trapped bunch length is $L_b = 6.3$ μm (21 fs) and 60% of the electrons are contained within 66 MeV $\pm 8\%$. Figure 3 summarizes simulations in which the injection pulse amplitudes $a_{1m} = a_{2m}$ were varied. Parameters are the same as in Fig. 2 except that $\psi_1 = -13.8$ and $\psi_2 = 21.5$. This ψ_1 value was carefully chosen so as to minimize the value of a_{1m} required for injection and agrees well with the analytical prediction ($\psi_1 = -1.3 - 2\pi j = -13.87$ for $j = 2$). Plotted as functions of a_{1m} are the maximum u_{zm}, average $\langle u_z \rangle$, and spread $\delta u_z/\langle u_z \rangle$, in the momenta, and the fraction f_{tr} of those particles which encounter the
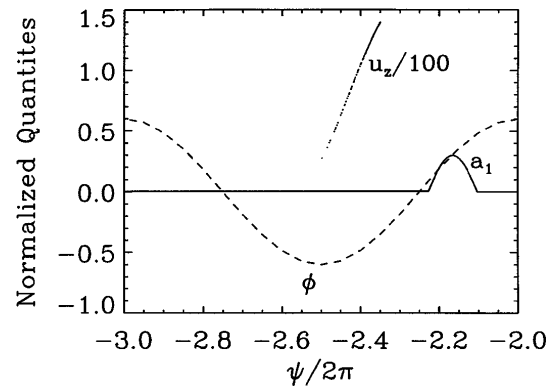

FIG. 2. Trapped electron phase space u_z versus ψ at $\tau = 300$ from a simulation with $\omega_1/\omega_p = 100$, $\omega_2/\omega_p = 90$, $\phi_0 = 0.6$, $a_{1m} = a_{2m} = 0.3$, and $L_1 = L_2 = \lambda_p/8$. Also shown are the injection pulse $\hat{a}_1$ (solid curve) and wake ϕ (dashed curve).

beat wave that become trapped. Trapping is observed for $a_{1m} > 0.17$, somewhat higher than the analytical prediction (0.11). Additional simulations indicate that trapping occurs when the center of the $L_1 = \lambda_p/8$, $a_{1m} = 0.3$ pulse is located within $-14.2 \leq \psi_1 \leq -13.5$. This implies that the forward pulse must be synchronized to the wake with an accuracy < 37 fs, which is not a serious constraint and can be relaxed somewhat by using a longer forward pulse. Furthermore, simulations show that $\langle u_z \rangle$ and $\delta u_z/\langle u_z \rangle$ are relatively insensitive to variations in $L_{1,2}$. The observed momentum spread can be traced to the half-sine pulse profiles, which implies that different electrons encounter different beat wave amplitudes and are injected into the wake with different energies.

Important 3D beam dynamics issues—in particular, the effect of the radial electric wake field E_r—have been addressed with the 1D simulation model. The wake potential for a pump laser pulse with a Gaussian radial profile is $\phi \simeq \phi_0 \exp(-2r^2/r_0^2) \cos\psi$, where r_0 is the laser spot size. This implies that the radial electric field acting upon the trapped electrons will be focusing for
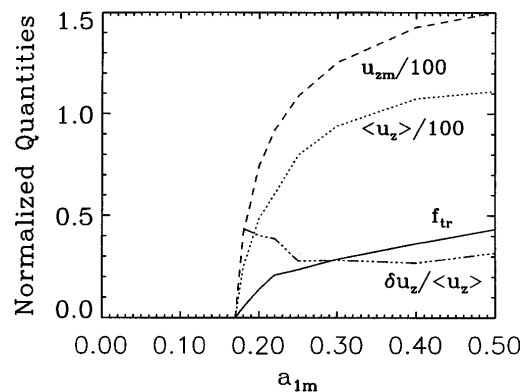

FIG. 3. The maximum u_{zm}, average $\langle u_z \rangle$, and spread $\delta u_z/\langle u_z \rangle$ in the momenta, and the fraction f_{tr} of trapped electrons as functions of $a_{1m} = a_{2m}$, for the parameters of Fig. 2 with $\psi_1 = -13.8$.
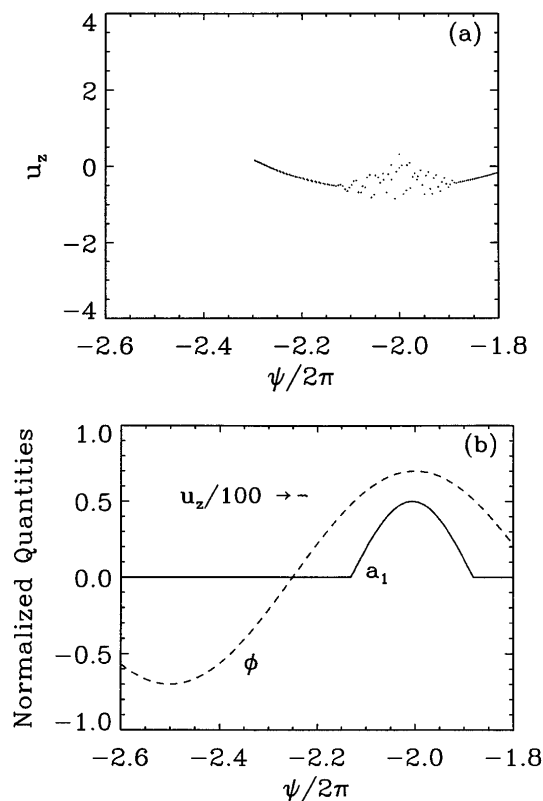
FIG. 4. Electron phase space u_z versus ψ (a) during the collision $\tau = 21$ and (b) after the collision $\tau = 100$ from a simulation with $\omega_1/\omega_p = 100$, $\omega_2/\omega_p = 85$, $\phi_0 = 0.7$, $a_{1m} = a_{2m} = 0.5$, and $L_1 = L_2/4 = \lambda_p/4$. Shown in (b) are the trapped electron bunch (located by arrow), the injection pulse $\hat{a}_1$ (solid curve), and wake ϕ (dashed curve) profiles.

$\cos\psi > 0$ and defocusing for $\cos\psi < 0$. For the near-threshold cases presented thus far, electrons which were initially injected within the focusing region of the wake slipped back into a defocusing region before they became highly relativistic. This is not the case in Fig. 4, which presents a simulation in which the position of the injection pulse was moved slightly forward and both the duration and amplitude of the injection pulses were increased, i.e., $\psi_1 = -12.6$, $a_{1m} = a_{2m} = 0.5$, $\phi_0 = 0.7$, $L_1 = L_2/4 = \lambda_p/4$, $\omega_1/\omega_p = 100$, and $\omega_2/\omega_p = 85$ ($\lambda_1 = 0.85$ μm, $\lambda_2 = 1$ μm, and $\lambda_p = 85$ μm). The electrons were injected at an earlier phase position with slightly higher energies and remained trapped in a focusing region of the wake. Plotted in Fig. 4 is the electron phase space (a) during the colliding pulse interaction at $\tau = 21$ and (b) after a distance of $\tau_{max} = 100$ (0.14 cm) with $\psi_{max} = 4$. Note that the front and back portions of the plasma electron segment in Fig. 4(a), which have not been significantly perturbed by the injection pulses, remain untrapped and have slipped out the back of Fig. 4(b). The results are quite dramatic: A bunch duration of 2.9 fs was obtained due to natural compression provided by the axial electric field, with a mean energy of 27 MeV and a standard deviation in energy of 0.32%. The trapping fraction is $f_{tr} \simeq 19\%$ and the bunch density

is $n_b = 1.8 \times 10^{18}$ cm^{-3}. It should be noted that the electron slippage seen in Fig. 2 can be compensated by a slight decrease in the ambient density as a function of z. An appropriate reduction in $n_0(z)$ can increase the plasma wavelength such that the trapped electrons remain in the focusing region of the wake.

The bunch density is $n_b \simeq f_{tr} n_0 L_z/L_b$, where $L_z \simeq (L_1 + L_2)/2$ is the length of plasma that encounters the overlapping pulses. Assuming that the 1D results hold for a pump laser of radius r_0 implies a total number of trapped electrons $N_b \simeq f_{tr} n_0 L_z \pi r_0^2$, e.g., $N_b \simeq 7.7 \times 10^9$ for Fig. 4 with $r_0 = 40$ μm. Note that N_b can be increased by increasing n_0, r_0, a_{1m} (via f_{tr}) and, in particular, L_z by increasing the duration of the backward pulse L_2. The ratio of N_b to the theoretical beam loading limit N_0 [12] is $N_b/N_0 = f_{tr} k_p L_z E_0/E_z$, which can easily approach unity. For N_b near N_0, however, space-charge effects become important and a self-consistent simulation is required.

[1] For a recent review, see E. Esarey et al., IEEE Trans. Plasma Sci. 24, 252 (1996).

[2] J. R. Marques et al., Phys. Rev. Lett. 76, 3566 (1996); C. W. Siders et al., Phys. Rev. Lett. 76, 3570 (1996); A. Ting et al., Phys. Rev. Lett. 77, 5377 (1996); S. P. LeBlanc et al., Phys. Rev. Lett. 77, 5381 (1996).

[3] K. Nakajima et al., Phys. Rev. Lett. 74, 4428 (1995); C. Coverdale et al., Phys. Rev. Lett. 74, 4659 (1995); A. Modena et al., Nature (London) 377, 606 (1995); D. Umstadter et al., Science 273, 472 (1996).

[4] A. Ting et al., Phys. Plasmas 4, 1889 (1997).

[5] T. Tajima and J. M. Dawson, Phys. Rev. Lett. 43, 267 (1979); P. Sprangle et al., Appl. Phys. Lett. 53, 2146 (1988); L. M. Gorbunov and V. I. Kirsanov, Sov. Phys. JETP 66, 209 (1987).

[6] P. Sprangle et al., Phys. Rev. Lett. 69, 2200 (1992); T. M. Antonsen and P. Mora, Phys. Rev. Lett. 69, 2204 (1992); N. E. Andreev et al., JETP Lett. 55, 571 (1992); E. Esarey et al., Phys. Fluids B 5, 2690 (1993).

[7] E. Esarey, J. Krall, and P. Sprangle, Phys. Rev. Lett. 72, 2887 (1994); W. B. Mori et al., Phys. Rev. Lett. 72, 1482 (1994); N. E. Andreev, V. I. Kirsanov, and L. M. Gorbunov, Phys. Plasmas 2, 2573 (1995).

[8] D. Umstadter, J. K. Kim, and E. Dodd, Phys. Rev. Lett. 76, 2073 (1996).

[9] C. Joshi et al., Phys. Rev. Lett. 47, 1285 (1981); D. W. Forslund et al., Phys. Rev. Lett. 54, 558 (1985).

[10] P. Bertrand et al., Phys. Rev. E 49, 5656 (1994); Phys. Plasmas 2, 3115 (1995).

[11] E. Esarey and M. Pilloff, Phys. Plasmas 2, 1432 (1995).

[12] T. Katsouleas et al., Part. Accel. 22, 81 (1987).